Transverse momentum spectra in high-energy nucleus-nucleus, proton-nucleus and proton-proton collisions*

XIE Wen-Jie(谢文杰)[1)]

Department of Physics, Yuncheng University, Yuncheng 044000, China

Abstract: The transverse momentum distributions of final-state particles produced in nucleus-nucleus (AA), proton-nucleus (pA), and proton-proton (pp) collisions at high energies are investigated using a multisource ideal gas model. Our calculated results show that the contribution of hard emission can be neglected in the study of transverse momentum spectra of charged pions and kaons produced in Cu-Cu collisions at $\sqrt{s_{\rm NN}}$=22.5 GeV. And if we consider the contribution of hard emission, the transverse momentum spectra of p and $\bar{\rm p}$ produced in Cu-Cu collisions at $\sqrt{s_{\rm NN}}$=22.5 GeV, $\rm K^0_s$ produced in Pb-Pb collisions at 158 A GeV, J/ψ particles produced in p-Pb collisions at 400 GeV and π^+, $\rm K^+$, p produced in proton-proton collisions at $\sqrt{s}$=200 GeV, can be described by the model, especially in the tail part of spectra.

Key words: transverse momentum spectra, multisource ideal gas model, final-state particles, Cu-Cu, Pb-Pb p-Pb, p-p collisions

PACS: 25.75.Dw, 24.10.Pa **DOI:** 10.1088/1674-1137/35/12/006

1 Introduction

The study of distribution laws of final-state paticles produced in high-energy nucleus-nucleus (AA), proton-nucleus (pA) and proton-proton (pp) collisions is an important subject in particle and nucleus physics. These distributive laws including the transverse and longitudinal direction can provide information on the production process.

Much experimental data of nucleus-nucleus collisions at high energies were reported in the past years [1–4]. To explain these experimental data, many theoretical models were proposed [5–16]. Most of these models are dynamical microscopic models and thermal models. To study the particle productions in a wider energy range, the PHENIX collaboration measured the transverse momentum distributions of particles produced in Cu-Cu collisions at center–of-mass energy $\sqrt{s_{\rm NN}}$=22.5 GeV [17]. The BRAHMS collaboration measured the transverse momentum distributions of particles produced in p-p collisions at center-of-mass energy $\sqrt{s_{\rm NN}}$=200 GeV [18]. The NA50 collaboration measured the transverse momentum distributions of J/ψ particles produced in p-Pb collisions at 400 GeV [19] and the NA49 collaboration measured the transverse momentum spectra of $\rm K^0_S$ produced in central Pb-Pb collisions at 158 A GeV [20]. It is very interesting to analyze these experimental data using a theoretical model.

A few modeling or empirical formulas are used in describing the transverse momentum and transverse mass distribution [21–24]. Thermal models are attractive because they predict all particle abundances by using three parameters, namely temperature, the baryochemical potential and the volume of the fireball. In this paper, we will use and develop the multisource ideal gas model [25–30] and give a description of the transverse momentum distributions of final-state particles produced in Cu-Cu, Pb-Pb, p-Pb and p-p collisions at high energies.

Received 6 March 2011

* Supported by National Natural Science Foundation of China (10975095) and Natural Science Foundation of Shanxi Province (2007011005)

1) E-mail: wenjiexie@yeah.net

2 The model

In AA, pA and pp collisions at high energies, the final-state particles will be produced by two processes, namely "the hard emission process" and "the soft emission process" [31].

The momentum values of the particles formed in the hard emission process are not less than 2.5 GeV/c. The momentum values of the particles formed in the soft emission process are less than 2.5 GeV/c. Generally speaking, the proportion of particles formed in the soft process is more than 99%. According to the multisource ideal gas model [25–30], a lot of emission sources of particles are formed in hard and soft emission processes in AA, pA and pp collisions at high energies. The degrees of excitation of the emission sources formed in the hard emission process are greater than the degrees of excitation of the emission sources formed in the soft emission process. A higher degree of excitation corresponds to a greater temperature value. We assume that there is a thermodynamic equilibrium or a local thermodynamic equilibrium at the time of freeze-out. All emission sources of the particles formed in the hard emission process have the same temperature, and all emission sources of particles formed in the soft emission process have the same temperature. As we neglect the particles formed in the hard emission process, all emission sources are assumed to be in thermodynamic equilibrium. The source number in the hard emission process is assumed to be $n_{\rm h}$ and the source number in the soft emission process is assumed to be $n_{\rm s}$. Each source contributes a transverse momentum distribution like a radioactive object.

The transverse momentum ($p_{{\rm T}i}$) distribution contributed by the ith source of the particles produced in a hard or soft emission is an exponential function, we have

$$f(p_{{\rm T}i})=\frac{1}{T_i}\exp\left(-\frac{p_{{\rm T}i}}{T_i}\right), \tag{1}$$

where T_i is the temperature of the ith source, which describes the degree of excitation of the emission source. As the emission sources produced in the hard process are in thermodynamic equilibrium, we have

$$T_1=T_2=\cdots=T_{n_{\rm h}}. \tag{2}$$

As for the emission sources produced in the soft process, we have

$$T_1=T_2=\cdots=T_{n_{\rm s}}. \tag{3}$$

The transverse momentum ($p_{\rm Th}$) distributions contributed by all emission sources from the hard emission process are the fold of $n_{\rm h}$ exponential functions, namely [25, 26]

$$f(p_{\rm Th})=\frac{p_{\rm Th}^{n_{\rm h}-1}}{(n_{\rm h}-1)!T_{\rm h}^{n_{\rm h}}}\exp\left(-\frac{p_{\rm Th}}{T_{\rm h}}\right), \tag{4}$$

where $T_{\rm h}$ is the temperature parameter which denotes the degree of excitation of the hard emission source. Similarly, transverse momentum ($p_{\rm Ts}$) distributions contributed by all emission sources from the soft emission process are the fold of $n_{\rm s}$ exponential functions, namely [25, 26]

$$f(p_{\rm Ts})=\frac{p_{\rm Ts}^{n_{\rm s}-1}}{(n_{\rm s}-1)!T_{\rm s}^{n_{\rm s}}}\exp\left(-\frac{p_{\rm Ts}}{T_{\rm s}}\right), \tag{5}$$

where $T_{\rm s}$ is a temperature parameter which denotes the degree of excitation of the soft emission source. And the total transverse momentum ($p_{\rm T}$) distributions contributed by all emission sources from both the soft and hard emission processes can be written as

$$\begin{aligned} f(p_{\rm T}) \;=\; & k\frac{p_{\rm T}^{n_{\rm s}-1}}{(n_{\rm s}-1)!T_{\rm s}^{n_{\rm s}}}\exp\left(-\frac{p_{\rm T}}{T_{\rm s}}\right) \\ & +(1-k)\frac{p_{\rm T}^{n_{\rm h}-1}}{(n_{\rm h}-1)!T_{\rm h}^{n_{\rm h}}}\exp\left(-\frac{p_{\rm T}}{T_{\rm h}}\right), \end{aligned} \tag{6}$$

where k is the relative weight contributed by the particles formed in the soft process.

To avoid the complex calculation in the analytical method, in this work we will use the Monte Carlo method to calculate the transverse momentum spectra. In the Monte Carlo calculation, according to Eq. (1), the transverse momentum ($p_{{\rm T}i}$) contributed by the ith source of particles produced in a hard or soft emission can be obtained by

$$p_{{\rm T}i}=-T_i\ln R_i(1), \tag{7}$$

where $R_i(1)$ stands for even random variables distributed in [0,1]. For the emission sources from the hard and soft processes, according to Eqs. (4) and (5), we have

$$p_{\rm Th}=-\sum_{i=1}^{n_{\rm h}}T_{\rm h}\ln R_i(1), \tag{8}$$

and

$$p_{\rm Ts}=-\sum_{i=1}^{n_{\rm s}}T_{\rm s}\ln R_i(1), \tag{9}$$

respectively. The transverse momentum distribution is finally obtained by a statistical method.

3 Results and comparisons

In Figs. 1–6, the transverse momentum distributions of the charged pions, charged kaons, proton and

Table 1. Parameter values for curves in Figs. 1–6. The units of $T_{\rm s}$, $T_{\rm h}$ and T' are GeV.

figure	parameter	minimum bias	0–10%	10%–30%	30%–60%	60%–100%
Fig. 1	$T_{\rm s}$	0.28	0.28	0.28	0.27	0.26
	T'	0.18	0.18	0.18	0.17	0.16
	$n_{\rm s}$	1	1	1	1	1
Fig. 2	$T_{\rm s}$	0.27	0.27	0.27	0.26	0.25
	T'	0.17	0.17	0.17	0.16	0.15
	$n_{\rm s}$	1	1	1	1	1
Fig. 3	$T_{\rm s}$	0.265	0.26	0.26	0.25	0.25
	T'	0.20	0.20	0.20	0.20	0.20
	$n_{\rm s}$	2	2	2	2	2
Fig. 4	$T_{\rm s}$	0.235	0.235	0.235	0.225	0.205
	T'	0.20	0.20	0.20	0.20	0.15
	$n_{\rm s}$	2	2	2	2	2
Fig. 5	$T_{\rm s}$	0.25	0.25	0.25	0.24	0.21
	$T_{\rm h}$	0.41	0.44	0.38	0.38	0.36
	T'	0.25	0.25	0.25	0.25	0.21
	$n_{\rm s}$	3	3	3	3	3
	$n_{\rm h}$	3	3	3	3	3
Fig. 6	$T_{\rm s}$	0.225	0.235	0.23	0.21	0.14
	$T_{\rm h}$	0.41	0.47	0.39	0.39	0.26
	T'	0.23	0.23	0.23	0.19	0.13
	$n_{\rm s}$	3	3	3	3	3
	$n_{\rm h}$	3	3	3	3	3

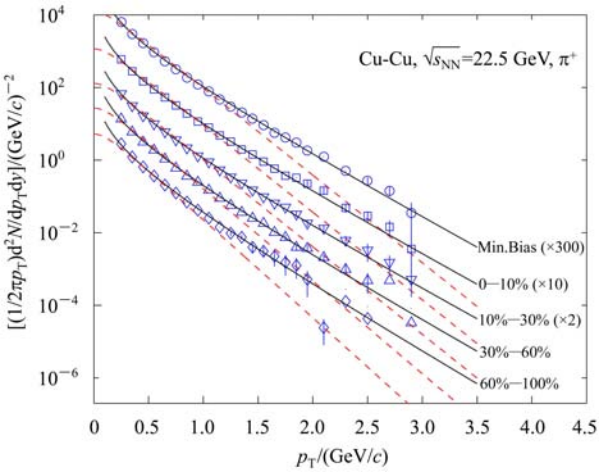

Fig. 1. The transverse momentum distributions of positively charged pions from Cu-Cu collisions at $\sqrt{s_{\rm NN}}$=22.5 GeV for four centrality classes and minimum bias sample. The symbols are the PHENIX experimental data [18]. The solid curves are our calculated results from Eq. (9) and the dashed curves are the results from Eq. (10). The spectra are shown for different centrality bins, with each one scaled by the amount indicated in the legend.

antiproton from the Cu-Cu collisions at $\sqrt{s_{\rm NN}}$= 22.5 GeV, for the four classes of centralities and minimum bias sample, are shown respectively. The experimental data are taken from the PHENIX collaboration [18] which are denoted by the symbols. The solid curves are the calculated results from Eqs. (8) and (9). The spectra for the 30%–60% and 60%–100% centrality bins, except for the p spectra, are shown unscaled, and for other centrality bins, the spectra are scaled by the amount indicated in the legend. The parameter values obtained by fitting the experimental data are displayed in Table 1. The χ^2-testing method is used in the selection of parameter values. For the charged pions and kaons, we neglect the contribution of the hard process. Namely, we take k=1 in Eq. (6). And for p and $\bar{\rm p}$ we take k=0.985. As a comparison, we use Eq. (6) with k=1 in the description of p and $\bar{\rm p}$ transverse momentum spectra, which are represented by the dashed curves.

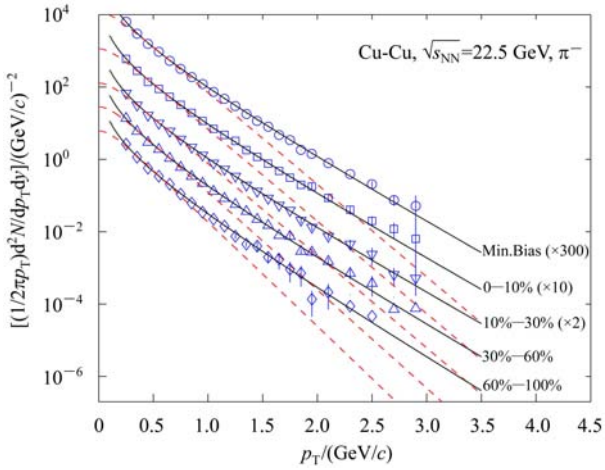

Fig. 2. The same as Fig. 1, but it shows the distributions of negatively charged pions.

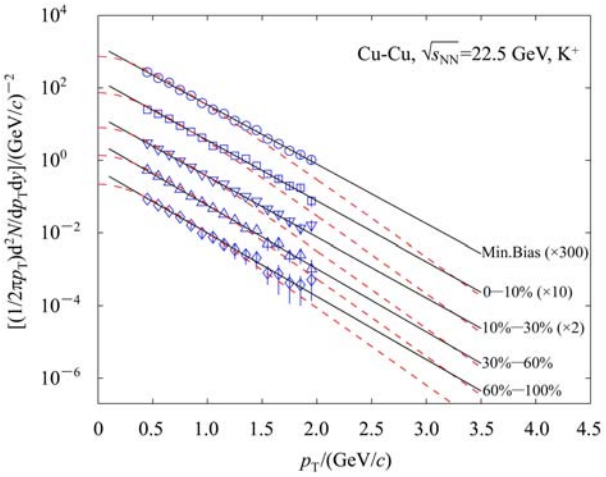

Fig. 3. The same as Fig. 1, but it shows the distributions of positively charged kaons.

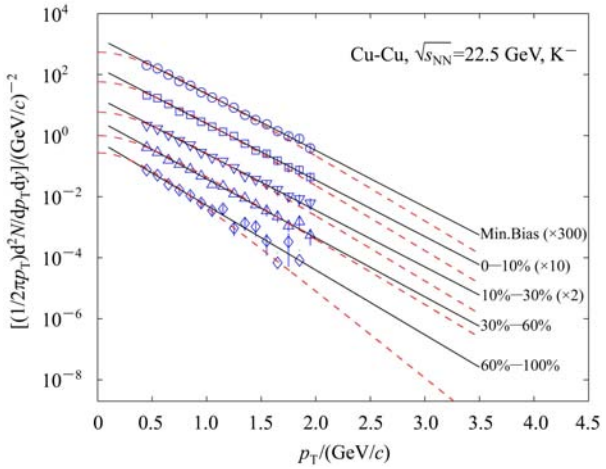

Fig. 4. The same as Fig. 1, but it shows the distributions of negatively charged kaons.

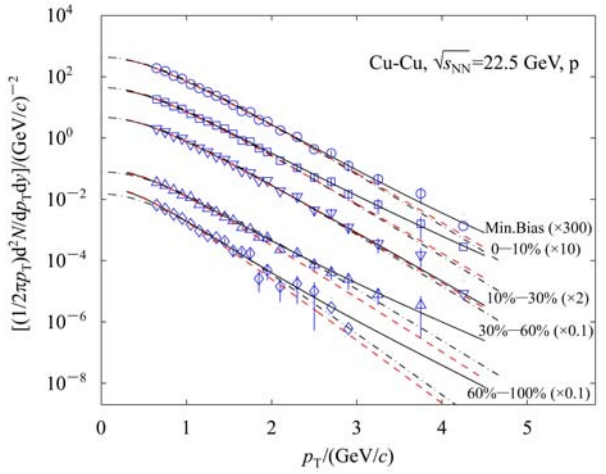

Fig. 5. The same as Fig. 1, but it shows the distributions of protons. The solid curves denote the results from Eqs. (8) and (9). The dashed curves are the results from Eq. (6) with k=1 and the dotted curves are the results from Eq. (10).

There is good parametrization of the transverse momentum distribution in Ref. [20], namely

$$\frac{\mathrm{d}N}{\mathrm{d}p_\mathrm{T}} = Cp_\mathrm{T}\exp\left(-\frac{\sqrt{p_\mathrm{T}^2+m_0^2}}{T'}\right), \tag{10}$$

where C is a normalization constant, m_0 is the rest mass of a particle, and T' is the temperature, which determines the width (σ) of the particle transverse momentum distribution. The relationship between T' and σ is [32]

$$\sigma^2 = m_0\bar{\gamma}T', \tag{11}$$

where $\bar{\gamma}$ is the mean Lorentz factor of the particles. In Figs. 1–4, we use the dashed curves to stand for the results from Eq. (10), and in Figs. 5 and 6 we use the dotted curves to show the calculated results from Eq. (10). From Figs. 1–6, we can see that Eq. (10) describes well the charged pions and kaons transverse momentum spectra in the lower transverse momentum regions but cannot describe them in the higher transverse momentum regions. From Figs. 5 and 6, there is a slight difference between Eq. (10) and Eq. (6) with k=1 in the description of p and $\bar{\mathrm{p}}$ transverse momentum spectra.

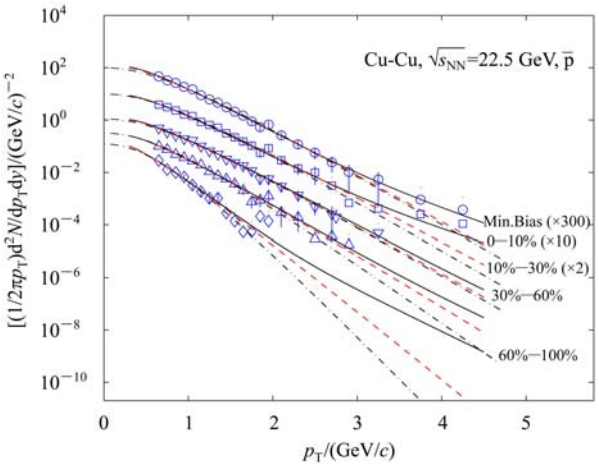

Fig. 6. The same as Fig. 1, but it shows the distributions of antiprotons. The solid curves denote the results from Eqs. (8) and (9). The dashed curves are the results from Eq. (6) with k=1 and the dotted curves are the results from Eq. (10).

The transverse momentum spectra of K_s^0 in three rapidity intervals in central Pb-Pb collisions at 158 A GeV are presented in Fig. 7. The symbols are the NA49 experimental data [20] and the solid curves are our calculated results by using Eqs. (8) and (9). The k value in Eq. (6) is 0.99, and the dashed curves

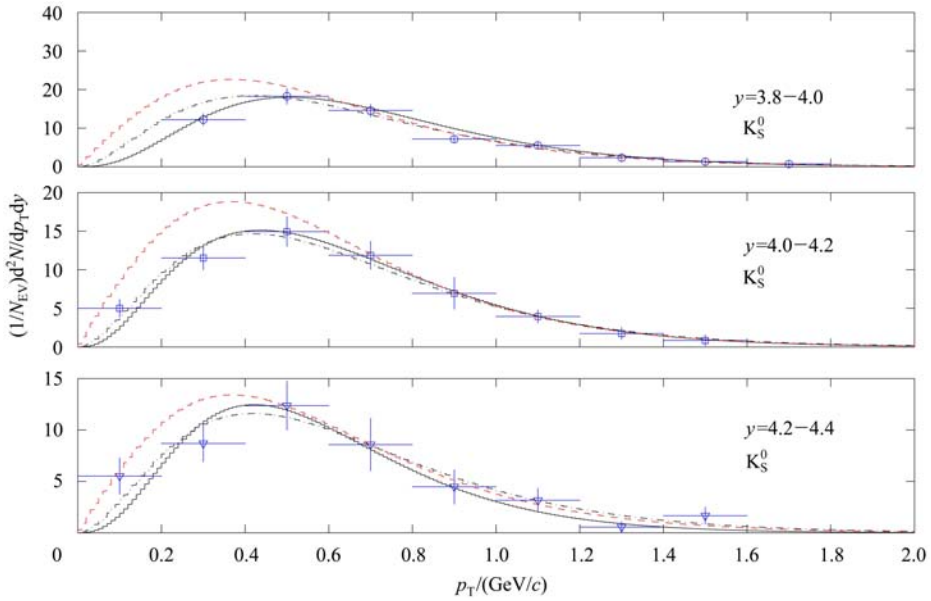

Fig. 7. Transverse momentum spectra of K_s^0, in three rapidity intervals, produced in central Pb-Pb collisions at 158 A GeV. The symbols are the NA49 experimental data [20]. The solid curves are our calculated results from Eqs.(8) and (9). The dashed curves are the results from Eq. (10) and the dotted curves are the results from Eq. (6) with $k=1$.

are the results from Eq. (10). The parameter values in the above two methods are shown in Table 2. The dotted curves are the results by using Eq. (6) with $k=1$. One can see that our calculated results are in agreement with the experimental data of the NA49 collaboration and Eqs. (8) and (9) are better than the other two methods in the description of K_s^0 transverse momentum spectra.

Table 2. Parameter values for curves in Fig. 7. The units of T_s, T_h and T' are GeV.

rapidity interval	T_s	T_h	T'	n_s	n_h
$3.8<y<4.0$	0.17	0.31	0.22	4	4
$4.0<y<4.2$	0.16	0.34	0.22	4	4
$4.2<y<4.4$	0.15	0.31	0.22	4	4

We show in Fig. 8 the transverse momentum distribution of J/ψ particles produced in p-Pb collisions at 400 GeV (the SPS energy). The data are taken from the NA50 collaboration [19], which are shown by the circles. The solid curves are our calculated results by Eqs. (8) and (9). The k value in Eq. (6) is 0.93 and in the calculation we take $n_s=3$, $n_h=2$, $T_s=0.39$ GeV and $T_h=0.59$ GeV. The dashed curves are the results from Eq. (6) with $k=1$ and in the calculation we take $n_s=3$ and $T_s=0.38$ GeV. The dotted curves are the results from Eq. (10) with $T'=0.29$ GeV. One can see that Eqs. (8) and (9) give a good description of J/ψ transverse momentum distributions, and both Eq. (6) with $k=1$ and Eq. (10) are no better than Eqs. (8) and (9) in the tail part of J/ψ transverse momentum spectra.

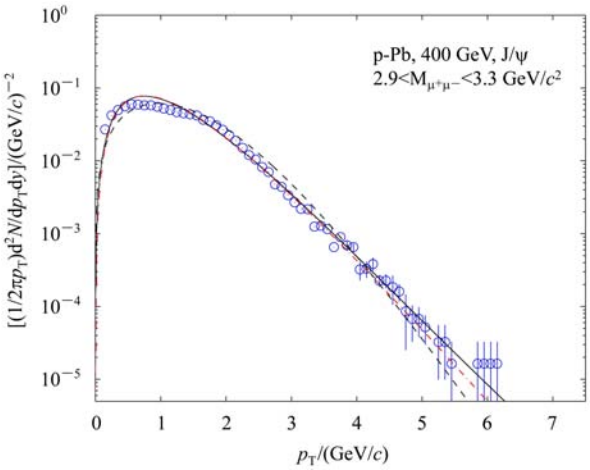

Fig. 8. Transverse momentum distribution of J/ψ particles produced in p-Pb collisions at 400 GeV. The circles are the experimental data of the NA50 collaboration [19]. The solid curves are our calculated results from Eqs. (8) and (9). The dashed curves are the results from Eq. (6) with $k=1$ and the dotted curves are the results from Eq. (10).

Figures 9, 10, and 11 represent the transverse momentum distributions of π^+, K^+ and p produced in pp collisions at $\sqrt{s}$=200 GeV (the RHIC energy) for seven rapidity intervals, respectively. The circles show the BRAHMS experimental data [18]. Our calculated results from Eqs. (8) and (9) are shown by

the solid curves for π^+, K^+ and p. The k value in Eq. (6) is 0.95. The dotted curves are our calculated results from Eq. (10). The parameter values in the above two methods are displayed in Table 3. As a comparison, we use Eq. (6) with k=1 to describe the transverse momentum spectra of π^+, K^+ and p from pp collisions at $\sqrt{s}$=200 GeV, which are indicated by the dashed curves. One can see again that our calculated results by using Eqs. (8) and (9) are better than the other two methods in the tail part of π^+, K^+ and p transverse momentum spectra.

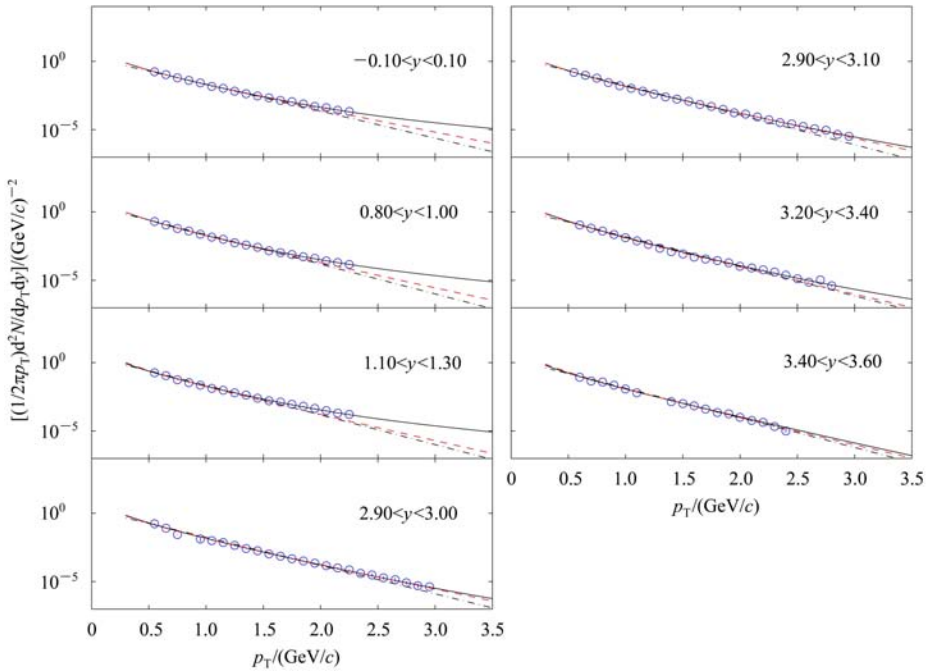

Fig. 9. Transverse momentum distributions of positively charged pions produced in pp collisions at $\sqrt{s}$=200 GeV for seven rapidity bins. The circles are the BRAHMS experimental data [18]. The solid curves are our calculated results from Eqs. (8) and (9). The dashed curves denote the results from Eq. (6) with $k=1$ and the dotted curves show the results from Eq. (10).

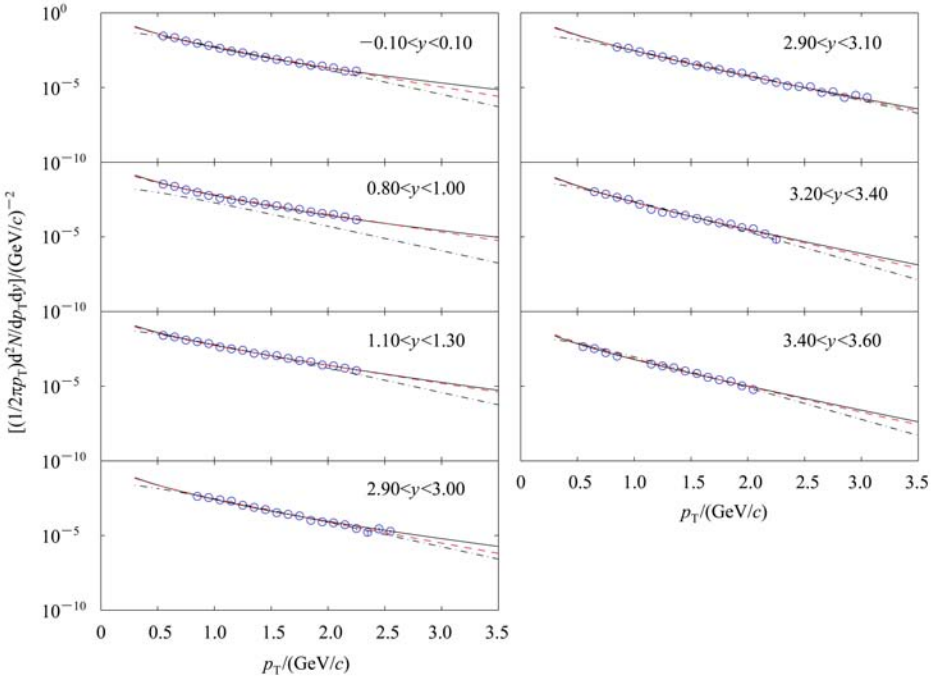

Fig. 10. The same as Fig. 9, but showing the distributions of positively charged kaons.

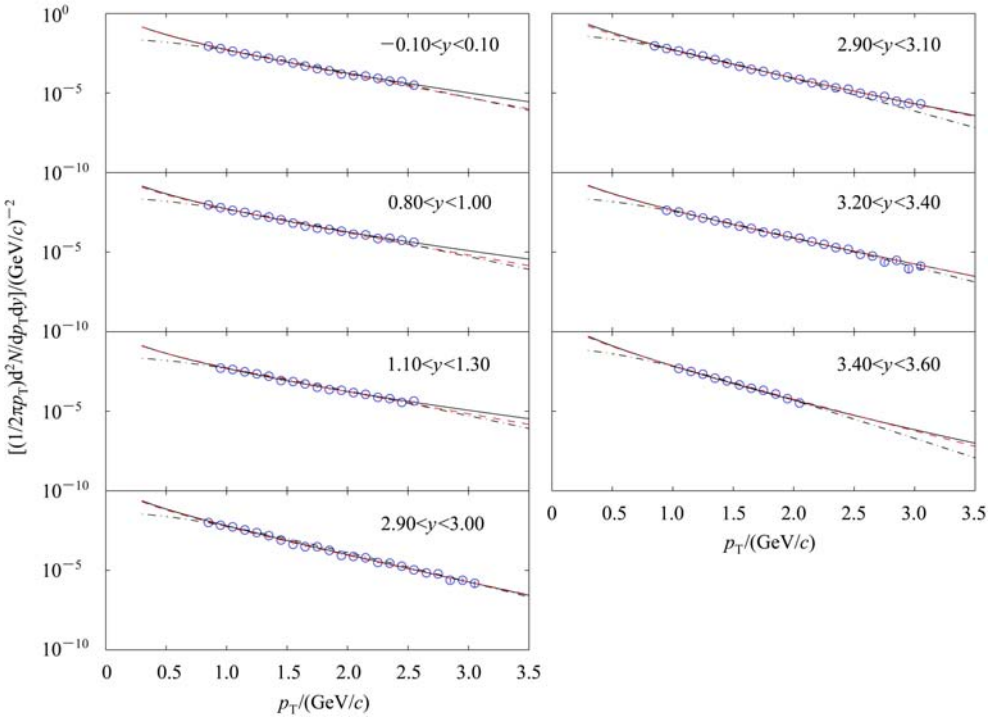

Fig. 11. The same as Fig. 9, but showing the distributions of protons.

Table 3. Parameter values for curves in Figs. 9–11. The units of T_s, T_h and T' are GeV.

particle	rapidity interval	T_s	T_h	T'	n_s	n_h
π^+	$-0.10 < y < 0.10$	0.285	0.59	0.22	1	2
	$0.80 < y < 0.90$	0.255	0.51	0.20	1	2
	$1.10 < y < 1.30$	0.265	0.53	0.20	1	2
	$2.90 < y < 3.00$	0.26	0.44	0.21	1	1
	$2.90 < y < 3.10$	0.255	0.43	0.20	1	1
	$3.20 < y < 3.40$	0.24	0.43	0.20	1	1
	$3.40 < y < 3.60$	0.25	0.30	0.20	1	1
K^+	$-0.10 < y < 0.10$	0.32	0.52	0.26	1	2
	$0.80 < y < 0.90$	0.34	0.53	0.26	1	2
	$1.10 < y < 1.30$	0.37	0.47	0.26	1	2
	$2.90 < y < 3.00$	0.30	0.44	0.26	1	2
	$2.90 < y < 3.10$	0.27	0.33	0.25	1	2
	$3.20 < y < 3.40$	0.25	0.32	0.20	1	2
	$3.40 < y < 3.60$	0.27	0.32	0.20	1	2
p	$-0.10 < y < 0.10$	0.31	0.42	0.26	1	2
	$0.80 < y < 0.90$	0.31	0.44	0.26	1	2
	$1.10 < y < 1.30$	0.31	0.44	0.26	1	2
	$2.90 < y < 3.00$	0.28	0.44	0.22	1	2
	$2.90 < y < 3.10$	0.28	0.38	0.20	1	1
	$3.20 < y < 3.40$	0.29	0.36	0.22	1	1
	$3.40 < y < 3.60$	0.22	0.31	0.17	1	1

Figures 12 and 13 show the dependence relationship between the transverse momentum distribution shape and the parameter values. The solid, dashed and dotted curves represent the transverse momentum distributions from Eq. (6) with different k values and the T_h, $0.9T_h$ and $1.1T_h$ values, respectively. From top to bottom, the T_h vlaues used in Fig. 11 are 0.42, 0.44, 0.44, 0.44, 0.38, 0.36 and 0.31 GeV for Fig. 12 and 0.31, 0.31, 0.31, 0.28, 0.28, 0.29 and 0.22 GeV for Fig. 13, respectively, and the k values are marked in the figure. The spectra are scaled by the amount displayed in the figure for clarity. From Fig. 12, we can see that, with increasing k from 0.00 to 0.98, the spectra in the middle and high trans-

verse momentum regions are sensitive to $T_{\rm h}$ and from Fig. 13, one can see that the transverse momentum distributions are insensitive to $T_{\rm s}$ when the k value is less than 0.95. The spectra in the middle and high transverse momentum regions are sensitive to $T_{\rm s}$ when the k value is increasing from 0.95 to 1.00.

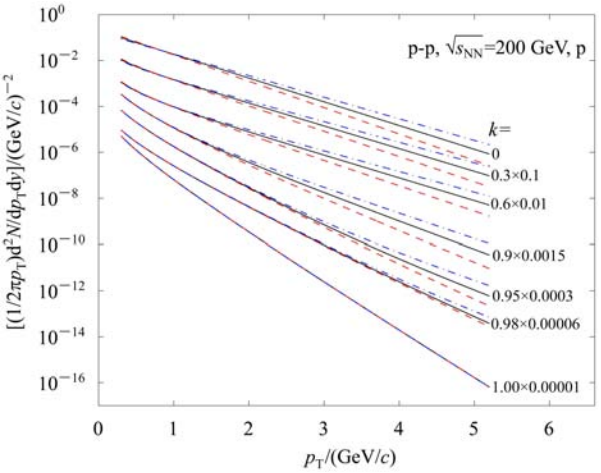

Fig. 12. The transverse momentum distributions of protons from Eq. (6) with different k values indicated in the figure and the $T_{\rm s}$ values used in Fig. 11. The solid, dashed and dotted curves represent the results with the $T_{\rm h}$, $0.9T_{\rm h}$ and $1.1T_{\rm h}$ values, respectively. The spectra are scaled by the amount indicated in the figure for clarity.

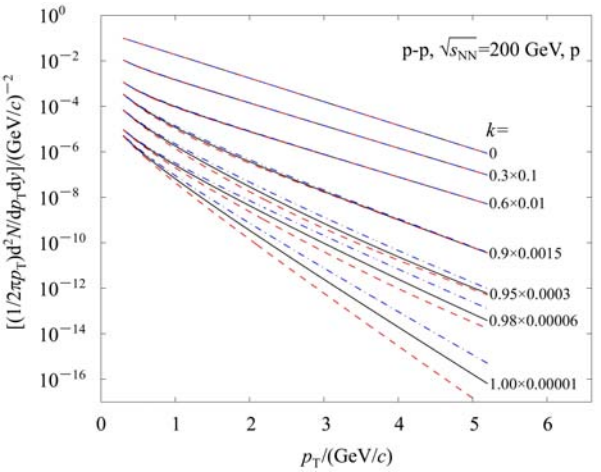

Fig. 13. The transverse momentum distributions of protons by using Eq. (6) with different k values indicated in the figure and the $T_{\rm h}$ values used in Fig. 11. The solid, dashed and dotted curves denote the calculated results with the $T_{\rm s}$, $0.9T_{\rm s}$ and $1.1T_{\rm s}$ values, respectively. The spectra are scaled by the amonut indicated in the figure for clarity.

4 Conclusions

In Table 1, we can see that the temperature parameters $T_{\rm s}$ and $T_{\rm h}$ decrease slightly with increasing centrality in Cu-Cu collisions at low RHIC energy. This means that the degree of excitation of the emission source decreases with increasing centrality and we know that a collision will be harder when a collision is a central collision. For p and $\bar{\rm p}$ produced in Cu-Cu collisions at the RHIC energy, the contribution of hard emission is very small. From Figs. 5 and 6, we know that, if we neglect the contribution of hard emission, the calculated results do not agree well with the experimental data in the tail part of the transverse momentum spectra.

In J/ψ transverse momentum distributions in p-Pb collisions at the SPS energy, the contribution of hard emission is small, too. In the region of $p_{\rm T} < 5$ GeV/c, the calculated results neglecting the hard emission describe well the experimental data. In pp collisions at high RHIC energy, the temperature parameters seem to be independent of the rapidity intervals and the values of the temperature parameters are greater than the values in Cu-Cu collisions at low RHIC energy and less than the values in p-Pb collisions at the SPS energy. The parameter k increases with increasing incident energy. This means that the contribution of hard emission increases with increasing incident energy.

In summary, the transverse momentum distributions of final-state particles produced in Cu-Cu collisions at low RHIC energy, Pb-Pb and p-Pb collisions at the SPS energy and pp collisions at the RHIC energy have been studied by the multisource ideal gas model. To avoid a complex calculation in the analytical method, a Monte Carlo method is used to calculate the transverse momentum spectra of concerned particles. Our calculations show that we can neglect the contributions of hard emission in the description of transverse momentum spectra of π^+, π^-, $\rm K^+$ and $\rm K^-$ produced in Cu-Cu collisions at $\sqrt{s_{\rm NN}}$=22.5 GeV, and for p and $\bar{\rm p}$ produced in Cu-Cu collisions at $\sqrt{s_{\rm NN}}$=22.5 GeV, π^+, $\rm K^+$, $\rm K^0_s$ produced in Pb-Pb collisions at 158 A GeV and J/ψ particles produced in p-Pb collisions at 400 GeV, p produced in pp collisions at $\sqrt{s}$=200 GeV, if we consider the contribution of hard emission the transverse momentum spectra of the above particles can be described by the model, especially in the tail part of spectra.

References

1 HONG B et al. (FOPI collaboration). Phys. Rev. C, 2005, **71**: 034902
2 EI-Nadi M, Ali-Mossa N, Abdelsalam A. Nuovo Cimento A, 1997, **110**: 1255
3 Kudzia D et al. Phys. Rev. C, 2003, **68**: 054903
4 Singh G, Sengupta K, Jain P L. Phys. Rev. C, 1990, **41**: 999
5 LI B A, Ko C M. Phys. Rev. C, 1995, **52**: 2037
6 Werner K. Z. Phys. C, 1989, **42**: 85
7 Capella A, Sukhatme U, TAN C I et al. Phys. Rep., 1994, **236**: 225
8 Bravina L V, Amelin N S, Csernai L P et al. Nucl. Phys. A, 1994, **544**: 461c
9 SA B H, TAI A. Phys. Rev. C, 1997, **55**: 2010
10 SA B H, TAI A. Phys. Lett. B, 1997, **399**: 29
11 Ehehalt W, Cassing W. Nucl. Phys. A, 1996, **602**: 449
12 Geiger K. Phys. Rep., 1995, **258**: 237
13 WANG X N, Gyulassy M. Phys. Rev. D, 1991, **44**: 3501
14 Westfall G D et al. Phys. Rev. Lett., 1976, **37**: 1202
15 Letessier J, Rafelski J, Tounsi A. Phys. Lett. B, 1992, **292**: 417
16 Braun-Munzinger P, Stachel J, Wessels J P et al. Phys. Lett. B, 1995, **344**: 43
17 Mitchell J T. (PHENIX collaboration). nucl-ex/0701079
18 YANG H Y. (BRAHMS collaboration). J. Phys. G, 2007, **34**: S619
19 Alessandro B, Alexa C, Arnaldi R et al. (NA50 collaboration). Eur. Phys. J. C, 2006, **48**: 329
20 Barnby L S. (NA49 collaboration). Ph. D. Thesis. University of Birmingham, 1999
21 Anticic T et al. (NA49 collaboration). Phys. Rev. C, 2004, **69**: 024902
22 Alt C et al. (NA49 collaboration). Phys. Rev. C, 2006, **73**: 044910
23 Antinori F et al. (NA57 collaboration). J. Phys. G, 2004, **30**: 823
24 Abelev B I et al. (STAR collaboration). Phys. Rev. C, 2009, **79**: 034909
25 LIU F H. Nucl. Phys. A, 2008, **810**: 159
26 LIU F H, LI J S. Phys. Rev. C, 2008, **78**: 044602
27 LIU F H. Europhys. Lett., 2003, **63**: 193
28 LIU F H, Abd Allah N N, ZHANG D H et al. Int. J. Mod. Phys. E, 2003, **12**: 713
29 LIU F H, Abd Allah N N, Singh B K. Phys. Rev. C, 2004, **69**: 057601
30 LIU F H. Can. J. Phys., 2004, **82**: 109
31 Adcox K et al. (PHENIX collaboration). Nucl. Phys. A, 2005, **757**: 184
32 Bhalla K B, Chaudry M, Lokanathan S et al. Nucl. Phys., A, 1981, **367**: 446